



## Evidence from neutron diffraction for superconductivity in the stabilized tetragonal phase of $\text{CaFe}_2\text{As}_2$ under uniaxial pressure

K. Prokeš,<sup>1,\*</sup> A. Kreyssig,<sup>2,3</sup> B. Ouladdiaf,<sup>4</sup> D. K. Pratt,<sup>2,3</sup> N. Ni,<sup>2,3</sup> S. L. Bud'ko,<sup>2,3</sup> P. C. Canfield,<sup>2,3</sup> R. J. McQueeney,<sup>2,3</sup> D. N. Argyriou,<sup>1</sup> and A. I. Goldman<sup>2,3</sup>

<sup>1</sup>*Helmholtz-Zentrum Berlin für Materialien und Energy, MI-1, Hahn-Meitner-Platz 1, 14109 Berlin, Germany*

<sup>2</sup>*Ames Laboratory, U.S. DOE, Iowa State University, Ames, Iowa 50011, USA*

<sup>3</sup>*Department of Physics and Astronomy, Iowa State University, Ames, Iowa 50011, USA*

<sup>4</sup>*Institut Laue-Langevin, 38042 Grenoble Cedex, France*

(Received 25 March 2010; published 12 May 2010)

$\text{CaFe}_2\text{As}_2$  single crystals under uniaxial pressure applied along the  $c$  axis exhibit the coexistence of several structural phases at low temperatures. We show that the room-temperature tetragonal phase is stabilized at low temperatures for pressures above 0.06 GPa, and its weight fraction attains a maximum in the region where superconductivity is observed under applied uniaxial pressure. Simultaneous resistivity measurements strongly suggest that this phase is responsible for the superconductivity in  $\text{CaFe}_2\text{As}_2$  found below 10 K in samples subjected to nonhydrostatic pressure conditions.

DOI: [10.1103/PhysRevB.81.180506](https://doi.org/10.1103/PhysRevB.81.180506)

PACS number(s): 74.70.Xa, 61.50.Ks, 74.62.Fj, 75.30.-m

Since their discovery, both the 1111 oxypnictide<sup>1</sup> and the 112 iron arsenide<sup>2</sup> superconducting families have undergone intensive scrutiny, particularly with respect to relationships between structure, magnetism, composition, and superconductivity (SC).<sup>3,4</sup> The parent  $R\text{FeAsO}$  ( $R$ =rare earth) and  $A\text{EFe}_2\text{As}_2$  ( $A\text{E}$ =Ca, Sr, and Ba) compounds are not superconductors at ambient pressure but undergo structural and antiferromagnetic (AF) transitions that are, at least in some instances, strongly coupled.<sup>3-6</sup> Upon chemical doping<sup>2,3</sup> or under pressure,<sup>7,8</sup> the structural and magnetic transitions are suppressed and SC is observed with  $T_C$  as high as 55 K.<sup>9</sup>

One of the most interesting anomalies in the  $A\text{EFe}_2\text{As}_2$  family is found in  $\text{CaFe}_2\text{As}_2$  under pressure as discussed in a recent review.<sup>4</sup> At ambient pressure,  $\text{CaFe}_2\text{As}_2$  undergoes a first-order transition from a high-temperature tetragonal ( $T$ ) phase ( $\text{ThCr}_2\text{Si}_2$  structure) to a structure with orthorhombic ( $O$ ) symmetry at  $T_{TO}=172$  K (Ref. 10) concomitant with an AF transition.<sup>6</sup> Upon the application of modest pressures, using liquid-media self-clamping cells, the structural and the AF transitions were rapidly suppressed and SC was observed for  $P \geq 0.23$  GPa and  $T \leq 12$  K.<sup>8,11</sup> SC has also been observed in electrical resistance measurements of samples under uniaxial pressure.<sup>12</sup>

Neutron powder-diffraction measurements, using a He-gas pressure cell to ensure hydrostatic pressure conditions, revealed a volume-collapsed tetragonal ( $cT$ ) phase in this pressure range, below  $\approx 100$  K.<sup>13</sup> Although the onset of SC seemed to be closely related to the appearance of the  $cT$  phase, more recent transport measurements under hydrostatic pressure conditions (He-gas cell) have revealed that neither the ambient pressure  $O$  phase (below  $T_{TO}$ ) nor the  $cT$  phase support SC.<sup>14</sup> These measurements along with an extended structural study by single-crystal neutron diffraction,<sup>15</sup> demonstrated that the electronic, magnetic, and structural transitions are sharp and clearly defined under hydrostatic pressure. Measurements done using a frozen liquid medium, in contrast, manifest a significant nonhydrostatic component upon the transition to the  $cT$  phase resulting in a low-temperature multicrystallographic-phase state that includes both the  $O$  and the  $cT$  phases among, perhaps, other as yet

unidentified phases. This is consistent with reports of the coexistence between static magnetic order and SC as inferred from muon spin rotation ( $\mu\text{SR}$ )<sup>16</sup> and recent nuclear magnetic resonance (NMR) experiments.<sup>17</sup> Nevertheless, the puzzle remains: which phase(s) is(are) responsible for SC in  $\text{CaFe}_2\text{As}_2$  under pressure? Does the orthorhombic phase support both superconductivity and magnetic ordering or, as speculated in Ref. 4, is SC associated with some residual untransformed  $T$  phase? Is SC to be found in this, as yet undiscovered phase at the boundary between the  $O$  and the  $cT$  phases?<sup>12,14,18</sup>

To investigate these issues, we have performed single-crystal neutron-diffraction measurements on  $\text{CaFe}_2\text{As}_2$  under uniaxial pressure. Since the  $c$  axis is subject to dramatic changes at the  $T$ - $cT$  transition, the uniaxial pressure was applied along this direction in an attempt to maximize the nonhydrostatic pressure component in a constrained geometry. For pressures above 0.06 GPa, we have observed diffraction from a structure (which we initially labeled  $T'$ ) that is consistent with the stabilization of the high-temperature tetragonal structure down to temperatures below the SC transition. We also find that with increasing applied pressures, the weight fraction of the  $T'$  and the  $cT$  phases increases at the expense of the  $O$  phase and the magnetically ordered fraction. This identifies the AF order with the  $O$  structure, consistent with previous studies.<sup>15</sup> Finally, *in situ* measurements of the in-plane ac resistivity (using the two-point contact method) clearly reveal the onset of SC below 10 K in our sample under uniaxial pressure. Taken together, this observation suggests that SC is hosted by the tetragonal phase which is stabilized under uniaxial pressure.

Several high-quality single crystals of  $\text{CaFe}_2\text{As}_2$  with masses between 8 and 12 mg, and dimensions of  $\approx 2-3$  mm  $\times$   $3-4$  mm  $\times$   $0.2$  mm were grown out of a Sn flux as described previously.<sup>10,13</sup> The crystals were gently polished to prepare flat and parallel surfaces perpendicular to the  $c$  axis. Neutron Laue exposures confirmed the good quality of samples after the polishing procedure. Crystals were subsequently clamped between two  $\text{ZrO}_2$  pistons that comprise a small uniaxial pressure cell<sup>19</sup> capable of applying up

to 1 kN of force on the sample. The pressure is calculated from the calibrated displacement of the clamping screws and the measured sample cross section. We have investigated five different single crystals at several pressures between ambient pressure and 0.3 GPa. It is important to note that the force produced by Bellville springs acts along the  $c$  axis of the sample, in strong contrast to hydrostatic or quasihydrostatic experiments, and maximizes the possibility to observe effects that were, in the literature, ascribed to nonhydrostatic conditions.<sup>4,12,14,15,18</sup> The pressure cell/sample system represents a confined geometry where thermal expansion and striction phenomena play an important role. Therefore, all pressure values mentioned below refer to those determined at room temperature. Perhaps most importantly, various structural phases (e.g., the  $T$ - $cT$  transition) that result in dimensional or volume changes cannot be regarded independently as they are mutually connected.

The neutron-diffraction experiments were performed on the E4 double-axis diffractometer at the Helmholtz-Zentrum Berlin using a neutron wavelength of  $\lambda=2.45$  Å and a standard cryostat. Additional data sets and measurements of the magnetic diffraction peaks were collected using the D10 diffractometer at the Institute Laue-Langevin (ILL) with a wavelength of 2.36 Å and a four-circle closed-cycle refrigerator capable of reaching temperatures down to 1.7 K. Both instruments make use of two-dimensional (2D) area detectors that provide a diffraction image over a range of scattering angles ( $2\theta$ ) as the sample is rocked over a specified angular range ( $\omega$ ). This considerably simplifies the task of mapping the evolution of the scattering with temperature [see Figs. 1(b)–1(e)]. Pyrolytic graphite filters were employed in both sets of measurements to reduce the higher harmonic contents to less than  $10^{-4}$  of the primary beam.

In Fig. 1(a), we show the temperature dependence of the signal in the vicinity of the  $(002)_T$  Bragg reflection measured on the E4 instrument with decreasing temperature. The nominal pressure applied along the  $c$  axis was 0.075 GPa. The actual 2D scan profiles recorded at 204, 145, 77, and 17 K are shown in Figs. 1(b)–1(e). As temperature is lowered below  $\approx 170$  K, the discontinuous change in the position of the bulk of the scattering to slightly lower scattering angle signals the  $T$ - $O$  transition.<sup>20</sup> However, besides the  $cT$  scattering signal at higher angle, there is a significant “tail” of scattering between signals originating from the  $O$  and the  $cT$  phases that persists down to at least 17 K (labeled  $T'$  in Fig. 1). Below  $\approx 100$  K, the intensity of the diffraction peak at this intermediate scattering angle decreases as the intensity of scattering from the  $cT$  phase increases. Several features of the  $T'$  diffraction peak in Fig. 1 are noteworthy: (a) it is clearly distinguishable from both the  $O$  and the  $cT$  phase peaks as temperature decreases, marking it as a different as yet unknown phase that coexists with the  $O$  and the  $cT$  phases at low temperatures; (b) there is no discernible discontinuity in the intensity or position of the  $T'$  diffraction peak as it evolves from the higher temperature  $(002)_T$  diffraction peak and; (c) the appearance and increase in the weight fraction of the  $cT$  phase and corresponding decrease in fraction (peak intensity) of the  $T'$  phase below  $\approx 100$  K is consistent with the temperature range of the  $T$ - $cT$  transition as measured by neutron diffraction under hydrostatic pres-

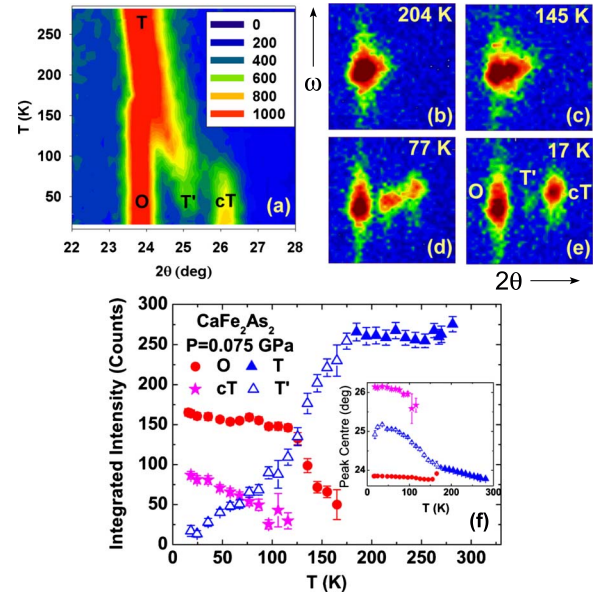


FIG. 1. (Color online) (a) Color map (counts per monitor are color coded in the inset) showing the temperature dependence of a portion of the diffraction pattern taken on the E4 diffractometer within the range of various structural  $(002)$  reflections of  $\text{CaFe}_2\text{As}_2$ . (b)–(e)  $2\theta$ - $\omega$  plots at selected temperatures showing the angular distribution of peaks tracked in (a). Panel (f) shows the temperature dependence of the integrated intensities and positions of reflections shown in panels (a)–(e).

sure conditions<sup>15</sup> and recent electrotransport measurements under uniaxial stress.<sup>12</sup> We, therefore, identify the  $T'$  diffraction peak as  $(002)_{T'}$  arising from some volume of the sample that has been stabilized in the high-temperature  $T$  phase due to the uniaxial pressure conditions. It is noteworthy that no trace of this stabilized  $T'$  phase was observed in neutron-diffraction measurements under hydrostatic pressure conditions.<sup>15</sup>

Following the measurement on E4, we investigated freshly polished  $\text{CaFe}_2\text{As}_2$  samples using the D10 instrument, which is equipped with a four-circle stage, to extend these measurements to other crystal orientations and characterize the magnetic scattering as well. Measurements at several pressures confirmed the picture described above including the emergence of the  $T'$  and the  $cT$  phases as the temperature was decreased below the  $T$ - $O$  transition. We also found, however, that this depends on the prior pressure history of the sample. Below a starting pressure of  $\approx 0.06$  GPa, the  $cT$  phase is absent at all temperatures and the  $T'$  phase is observed only over a narrow range of temperatures below  $T_{TO}$ . Upon increasing the pressure, we observe that the relative fractions of the stabilized tetragonal ( $T'$ ) and  $cT$  phases increase at the expense of the  $O$  phase, as would be expected from the  $p$ - $T$  phase diagram in reference.<sup>15</sup> A finite weight fraction of the  $T'$  phase extends down to the lowest temperatures measured for uniaxial pressures greater than 0.075 GPa. At even higher applied pressure, the  $cT$  phase appears at progressively higher temperatures and its weight fraction increases together with that of the  $T'$  phase at the expense of the  $O$  phase. For pressures in excess of  $\approx 0.27$  GPa, the relative fraction of  $T'$  decreases [see Fig. 3(c) inset]. The

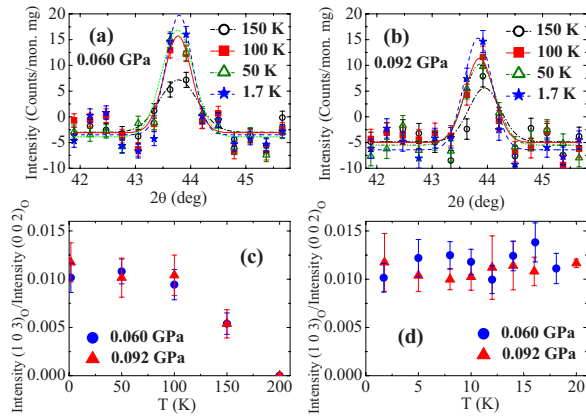


FIG. 2. (Color online) Representative examples of the magnetic diffraction peak observed at the  $(\frac{1}{2} \frac{1}{2} 3)_T$  [or  $(1 0 3)_O$ ] position obtained from two  $\text{CaFe}_2\text{As}_2$  samples using the D10 instrument under uniaxial pressures of (a) 0.060 GPa and (b) 0.092 GPa applied along the  $c$  axis (normalized to the same monitor and crystal weight). Line through the data represents fits using a single Gaussian. (c) The temperature dependence of the integrated intensities of data shown in (a) and (b) normalized to the intensity of the  $(002)_O$  reflections at the corresponding temperatures and pressures. (d) The normalized integrated intensities of the magnetic reflections in the vicinity of the expected superconducting transition (at  $\approx 10$  K) for  $P=0.060$  and 0.092 GPa.

lattice constants of the  $T'$  phase in the low-temperature limit at 0.092 GPa were determined from the D10 data to be  $a = 3.82(8)$  Å and  $c = 11.44(5)$  Å. Since the data set was limited by strong absorption of the cell and overlapping reflections from the  $O$  phase, a full structural refinement of the  $T'$  phase could not be performed.

In Figs. 2(a) and 2(b), we show representative diffraction profiles of the strongest magnetic reflection  $(\frac{1}{2} \frac{1}{2} 3)_T$ , [or  $(1 0 3)_O$ , in the  $O$  unit-cell notation]. These data were taken on two  $\text{CaFe}_2\text{As}_2$  samples on the D10 instrument under uniaxial pressures of 0.060 GPa and 0.092 GPa applied along the  $c$  axis, respectively. For comparison, the profiles were normalized to the same monitor and crystal weight. Figures 2(c) and 2(d) display the temperature and pressure dependence of fits to the data shown in Figs. 2(a) and 2(b) and reveal several important clues regarding the magnetism and SC in  $\text{CaFe}_2\text{As}_2$ . First, we note that the normalized integrated intensities taken at starting pressures of 0.060 and 0.092 GPa are essentially indistinguishable. Using the  $(002)_O$  nuclear peak for normalization, we estimate an ordered moment of  $0.8(1)\mu_B$  in good agreement with data in the literature. Second, within the given sensitivity limit of about  $0.2\mu_B$ , we found no evidence of magnetic ordering within the  $T'$  phase at any of the temperatures and pressures investigated. Together, this means that the magnetic scattering intensity at each pressure is simply proportional to the fraction of the  $O$  phase and there is no change in the magnetic-moment value in the  $O$  phase with increasing pressure, consistent with previous results from measurements under hydrostatic pressure.<sup>15</sup> We also point out that elastic<sup>15</sup> and inelastic<sup>21</sup> neutron-scattering measurements of under hydrostatic pressure have noted the absence of both a static ordered moment and low-energy spin fluctuations in the  $cT$

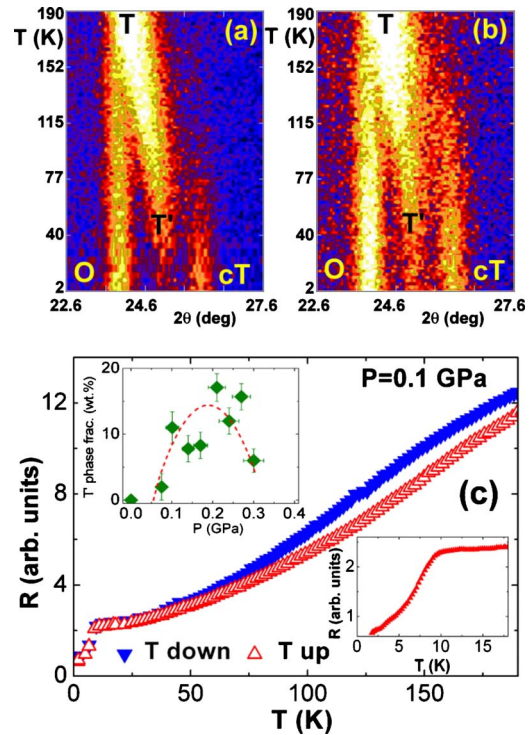


FIG. 3. (Color online) Color map showing the temperature dependence of a portion of the diffraction pattern taken at E4 in that covers various structural  $(002)$  reflections of  $\text{CaFe}_2\text{As}_2$  under uniaxial pressure of 0.1 GPa along the  $c$  axis measured with (a) decreasing and (b) increasing temperature. While the intensity in panel (a) is color-coded in the range 60–260, the (b) panel is in the range 60–220. The simultaneously measured electrical resistance is shown in panel (c). The lower inset to (c) shows the low-temperature detail of the electrical resistance data taken upon heating. The upper inset shows the weight fraction of the pressure stabilized phase  $T'$  as a function of applied pressure. The dotted line is a guide to the eyes.

phase. Finally, focusing our attention on Fig. 2(d), we find no evidence of suppression of the magnetic ordering at these pressures below the onset of SC as has been observed, for example, in recent measurements on doped  $\text{Ba}(\text{Fe}_{1-x}\text{Co}_x)_2\text{As}_2$  superconducting samples.<sup>22,23</sup> These data, then, are consistent with the identification of the AF ordering with the  $O$  phase and the absence of SC in the  $O$  phase for these samples. For the latter point, however, it is important to establish whether these samples under applied uniaxial pressure are, indeed, superconducting.

Figures 3(a) and 3(b) display the temperature dependence of the diffraction near the  $(002)_T$  Bragg reflection measured on the E4 instrument with (a) decreasing and (b) increasing temperature. The nominal pressure applied along the  $c$  axis in the present case was 0.1 GPa. Simultaneously, we measured the temperature dependence of the ac in-plane electrical resistivity using a two-point probe and the results are shown in Fig. 3(c) with the low-temperature detail magnified in the lower inset. From these data, we see that the onset of SC is clearly visible just below 10 K, although the resistivity does not reach zero even at 1.7 K. It is well known, however, that the two-point method always senses the residual contact resistivity and the measured values are greater than zero at



all temperatures. From the relevant (002) reflection intensities, we estimate the weight fraction of the  $T'$  phase at the lowest temperature to be  $\approx 10$  wt %. We note that the resistivity curve does not exhibit any sharp anomaly near the  $T$ - $O$  transition and, overall, is reminiscent of the data taken under uniaxial pressure ( $\approx 0.14$ – $0.17$  GPa) by Torikachvili *et al.*<sup>12</sup> By performing analogous diffraction experiments at different applied pressures, we have completed the pressure dependence of the weight fraction of the  $T'$  phase, which is shown in the upper inset of Fig. 3(c). The onset of SC (Ref. 12) occurs coincident with the first appearance of the  $T'$  phase. Unfortunately, the maximum uniaxial pressure attainable in our measurements is below that required for the offset of SC.

Summarizing our results on  $\text{CaFe}_2\text{As}_2$ : for applied uniaxial pressures above 0.060 GPa, one induces the  $cT$  phase which appears at progressively higher temperatures and the  $T'$  phase that, for applied pressures  $0.075 < P < 0.3$  GPa, is stabilized down to the lowest temperature measured (1.7 K). We propose that the critical factor for SC in  $\text{CaFe}_2\text{As}_2$  in both uniaxial and frozen medium pressure measurements is the stabilization of the tetragonal phase at low temperatures. Our observations correspond very well with the appearance of the superconducting dome as a function of the uniaxial pressure as observed by Torikachvili *et*

*al.*<sup>12</sup> The uniaxial pressure necessary to make  $\text{CaFe}_2\text{As}_2$  superconducting is about an order of magnitude lower than nominal “hydrostatic” pressure values produced by liquid medium clamping cells, i.e., approximately of the same order of magnitude as the nonhydrostatic component in the clamped cells. Although it is conceivable that SC is hosted by some other, as yet undetected additional phase, or through some strong modification of the  $O$  or the  $cT$  phase behavior that is not found under hydrostatic pressure conditions, we view this as unlikely in light of the consistent observation of SC in liquid-media pressure cells independent of the sample preparation methods. Finally, we note that the superconducting “bubble” observed for  $\text{CaFe}_2\text{As}_2$  extends over only a relatively narrow range of pressure (vanishingly small for the hydrostatic pressure measurements). This is consistent with our picture since with increasing pressure (at pressures where the  $O$  phase is suppressed), the fraction balance between the  $T$  and the  $cT$  phases changes in favor of the  $cT$  phase. At high enough pressures, the entire sample transforms to the nonsuperconducting  $cT$  phase.

We gratefully acknowledge the HZB and ILL for the allocated beam time and their support for this work. The work at the Ames Laboratory was supported by the U.S. DOE under Contract No. DEAC02-07CH11358.

\*prokes@helmholtz-berlin.de

- <sup>1</sup>Y. Kamihara, H. Hiramatsu, M. Hirano, R. Kawamura, H. Yanagi, T. Kamiya, and H. Hosono, *J. Am. Chem. Soc.* **128**, 10012 (2006).
- <sup>2</sup>M. Rotter, M. Tegel, and D. Johrendt, *Phys. Rev. Lett.* **101**, 107006 (2008).
- <sup>3</sup>Y. Ishida, F. Nakai, and H. Hosono, *J. Phys. Soc. Jpn.* **78**, 062001 (2009).
- <sup>4</sup>P. C. Canfield, S. L. Bud'ko, N. Ni, A. Kreyssig, A. I. Goldman, R. J. McQueeney, M. S. Torikachvili, D. N. Argyriou, G. Luke, and W. Yu, *Physica C* **469**, 404 (2009).
- <sup>5</sup>C. Krellner, N. Caroca-Canales, A. Jesche, H. Rosner, A. Ormeci, and C. Geibel, *Phys. Rev. B* **78**, 100504(R) (2008).
- <sup>6</sup>A. I. Goldman, D. N. Argyriou, B. Ouladdiaf, T. Chatterji, A. Kreyssig, S. Nandi, N. Ni, S. L. Bud'ko, P. C. Canfield, and R. J. McQueeney, *Phys. Rev. B* **78**, 100506(R) (2008).
- <sup>7</sup>H. Takahashi, K. Igawa, K. Arii, Y. Kamihara, M. Hirano, and H. Hosono, *Nature (London)* **453**, 376 (2008).
- <sup>8</sup>M. S. Torikachvili, S. L. Bud'ko, N. Ni, and P. C. Canfield, *Phys. Rev. Lett.* **101**, 057006 (2008).
- <sup>9</sup>Z. A. Ren, W. Lu, J. Yang, W. Yi, X.-L. Shen, Z. C. Li, G. C. Che, X. L. Dong, L. L. Sun, F. Zhou, and Z. X. Zhao, *Chin. Phys. Lett.* **25**, 2385 (2008).
- <sup>10</sup>N. Ni, S. Nandi, A. Kreyssig, A. I. Goldman, E. D. Mun, S. L. Bud'ko, and P. C. Canfield, *Phys. Rev. B* **78**, 014523 (2008).
- <sup>11</sup>T. Park, E. Park, H. Lee, T. Klimczuk, E. D. Bauer, F. Ronning, and J. D. Thompson, *J. Phys.: Condens. Matter* **20**, 322204 (2008).
- <sup>12</sup>M. S. Torikachvili, S. L. Bud'ko, N. Ni, P. C. Canfield, and S. T. Hannahs, *Phys. Rev. B* **80**, 014521 (2009).
- <sup>13</sup>A. Kreyssig, M. A. Green, Y. B. Lee, G. D. Samolyuk, P. Zajdel, J. W. Lynn, S. L. Bud'ko, M. S. Torikachvili, N. Ni, S. Nandi, J. B. Leao, S. J. Poulton, D. N. Argyriou, B. N. Harmon, R. J. McQueeney, P. C. Canfield, and A. I. Goldman, *Phys. Rev. B*

**78**, 184517 (2008).

- <sup>14</sup>W. Yu, A. A. Aczel, T. J. Williams, S. L. Bud'ko, N. Ni, P. C. Canfield, and G. M. Luke, *Phys. Rev. B* **79**, 020511(R) (2009).
- <sup>15</sup>A. I. Goldman, A. Kreyssig, K. Prokeš, D. K. Pratt, D. N. Argyriou, J. W. Lynn, S. Nandi, S. A. J. Kimber, Y. Chen, Y. B. Lee, G. D. Samolyuk, J. B. Leão, S. J. Poulton, S. L. Bud'ko, N. Ni, P. C. Canfield, B. N. Harmon, and R. J. McQueeney, *Phys. Rev. B* **79**, 024513 (2009).
- <sup>16</sup>T. Goko, A. A. Aczel, E. Baggio-Saitovitch, S. L. Bud'ko, P. C. Canfield, J. P. Carlo, G. F. Chen, P. Dai, A. C. Hamann, W. Z. Hu, H. Kageyama, G. M. Luke, J. L. Luo, B. Nachumi, N. Ni, D. Reznik, D. R. Sanchez-Candela, A. T. Savici, K. J. Sikes, N. L. Wang, C. R. Wiebe, T. J. Williams, T. Yamamoto, W. Yu, and Y. J. Uemura, *Phys. Rev. B* **80**, 024508 (2009).
- <sup>17</sup>S.-H. Baek, H. Lee, S. E. Brown, N. J. Curro, E. D. Bauer, F. Ronning, T. Park, and J. D. Thompson, *Phys. Rev. Lett.* **102**, 227601 (2009).
- <sup>18</sup>H. Lee, E. Park, T. Park, V. A. Sidorov, F. Ronning, E. D. Bauer, and J. D. Thompson, *Phys. Rev. B* **80**, 024519 (2009).
- <sup>19</sup>J. Kamarád, M. Mihalik, V. Sechovský, and Z. Arnold, *High Press. Res.* **28**, 633 (2008).
- <sup>20</sup>S. Bud'ko, N. Ni, and P. Canfield, [arXiv:0907.2936](https://arxiv.org/abs/0907.2936) (unpublished).
- <sup>21</sup>D. K. Pratt, Y. Zhao, S. A. J. Kimber, A. Hiess, D. N. Argyriou, C. Broholm, A. Kreyssig, S. Nandi, S. L. Bud'ko, N. Ni, P. C. Canfield, R. J. McQueeney, and A. I. Goldman, *Phys. Rev. B* **79**, 060510(R) (2009).
- <sup>22</sup>D. K. Pratt, W. Tian, A. Kreyssig, J. L. Zarestky, S. Nandi, N. Ni, S. L. Bud'ko, P. C. Canfield, A. I. Goldman, and R. J. McQueeney, *Phys. Rev. Lett.* **103**, 087001 (2009).
- <sup>23</sup>A. D. Christianson, M. D. Lumsden, S. E. Nagler, G. J. MacDougall, M. A. McGuire, A. S. Sefat, R. Jin, B. C. Sales, and D. Mandrus, *Phys. Rev. Lett.* **103**, 087002 (2009).